PORO-VISCOELASTICITY MODELLING BASED ON UPSCALING QUASISTATIC FLUID-SATURATED SOLIDS[1]

Eduard Rohan†, Simon Shaw‡, John R. Whiteman‡

† European Centre of Excellence, NTIS New Technologies for Information Society,
Faculty of Applied Sciences, University of West Bohemia,
Univerzitní 22, 30614 Plzeň, Czech Republic,
rohan@kme.zcu.cz

‡ BICOM, Institute of Computational Mathematics, Brunel University,
Uxbridge UB8 3PH, England,
Simon.Shaw@brunel.ac.uk, John.Whiteman@brunel.ac.uk

Keywords: viscoelasticity; two-scale modelling; homogenization; fluid-saturated porous media; Biot model; perfusion; viscoelastic solid porous media; unconsolidated sands; well bore deformation.

ABSTRACT

In this paper quasistatic models are developed for the slow flow of compressible fluids through porous solids, where the solid exhibits fading memory viscoelasticity. Problems of this type are important in practical geomechanics contexts, for example in the context of fluid flow through unconsolidated reservoir sands, and of well bore deformation behaviour in gas and oil shale reservoirs, all of which have been studied extensively. For slow viscous fluid flow in the poro-viscoelastic media we are able to neglect the dynamic effects related to inertia forces, as well as the dissipation associated with the viscous flows. This is in contrast to the vast body of work in the poro-elastic context, where much faster flow of the viscous fluids may give rise to *memory effects* associated with microflows in pores of the solid media. Such problems have been treated extensively in both the dynamic and quasistatic cases.

We are taking a specific type of the porous medium subject to slow deformation processes possibly inducing moderate pressure gradients and flow rates characterized by negligible inertia effects. As the result of homogenization of such a two phase medium, we observe the fading memory behaviour in the Biot modulus which controls the pressure increase due to skeleton macroscopic deformation and pore fluid content.

Although our derivation leads to a result which is consistent with the formal phenomenological approach proposed by Biot (1962), we offer the reader more insight into the structure of the poro-viscoelastic constitutive relations obtained; in particular, we can show that the Biot compressibility evolves in time according to the creep function while the skeleton stiffness is driven by the relaxation function.

1 Introduction

Problems of slow flow of compressible fluids in poro-viscoelastic media occur frequently in practical geomechanics and are currently important to the understanding and management

[1]BICOM report 12/2 at `www.brunel.ac.uk/bicom` (**version: February 11, 2014**)

of oil and gas reservoirs and of aquifers. As we shall argue below, examples of such problems are the viscoelastic deformation and creep of unconsolidated reservoir sands, and of clays, and of rock matrix deformation around boreholes in chalks and shales [31, 1, 24]. Much work has been devoted to modelling of flow and deformation in the oil/gas and water contexts and to experimental testing of these solid materials to obtain material parameters. As a result the effects of the viscoelastic rock deformation on the fluid flow are becoming better understood. The relevance of viscoelastic damping was also discussed recently in [9].

By way of illustration we now list a number of practical examples of this type of behaviour. Rago et al [31] produced a computational model of two-component slow fluid flow in viscoelastic porous media and used it to predict the recovery of solution gas from a geopresurised aquifer. Abousleiman et al [1] considered the mechanical creep and viscoelastic deformation of porous rock coupled with the hydraulic effects of fluid flow; their model was based on Biot's theory of poroelasticity, generalised to include the viscoelastic effects of the rock via the correspondence principle. The context considered was that of a borehole in the rocks, Berea sandstone, Danian chalk and deep water Gulf of Mexico shale and the significance of the viscoelastic effects was demonstrated. Again for wellbores Hoag et al [24] considered closure when drilling in gas shale and oil shale reservoirs. They investigated the effects of the shale matrix viscoelasticity on overall deformation behaviour of the wellbore, seeking to illustrate the instabilities that occur.

These references show that the problem of slow flow in viscoelastic porous media has important applications and that an assumption of quasistatic rock motion is appropriate. We note that these studies have usually taken the heuristic approach of adding the solid viscoelasticity effects through an assmption of a 'spring-dashpot' model or by invoking the *correspondence principle* (see e.g. [20]). A more general statement of the mathematical formluation does not seem to be available for this important class of problems and this is the main motivation behind the present work.

Considering now more generally the modelling of fluid flow in porous media, many difference scenarios arise and we identify two of the most relevant here. First, even without any macroscopically important fluid redistribution, the fading memory effect can be generated by microflows in media with the double porosity, see e.g. [4, 5, 38, 42].

Secondly, the fading memory which accompanies the deformation can arise from the presence of fluid transported through a porous elastic solid, as modelled originally by Biot in [7]. The approach taken there was based on the use of thermodynamics, energy and stress/strain relations for the elastic solid, together with a Darcy model for the fluid, to produce a mathematical formulation which involves history integrals and inertia terms. This work has since been revised and extended significantly using micromechanical approaches and asymptotic methods. The Darcy flow model with memory was derived in [28]. For acoustic problems, Ferrín and Mikelić in [18] (see also [19]) recovered the Biot equations with some additional memory effects arising from the fluid transport and fluid-structure interaction phenomena.

However, as alluded to above, we have in mind yet another situation where a *slow* fluid flow takes place in a viscoelastic solid in which the deformation is itself modelled using a conventional viscoelastic model based on a history integral. This type of viscoelastic deformation can therefore arise in situations where there is pressure but no fluid transport.

It is clear that in reality all these origins of memory effects may contribute but to deal with them all at once, here, would we believe be too cumbersome. For that reason we focus tightly on the extension of quasistatic poroelasticity to the case of a viscoelastic solid with slow flow. As far as we aware this is the first such derivation and formulation in the general

case.

The extension of the model of poroelasticity to include viscous effects must be done in a physically consistent way, such as using the Theory of Porous Media (TPM), [13, 16, 12], or using a direct upscaling procedure, see e.g. [29, 14]. The first approach of the TPM is based on the concept of volume fractions as the only condensed information about the microstructure. It was employed, e.g. by Ehlers [17], to study a biphasic description of viscoelastic foams. We shall pursue the second approach which uses more detailed information about a specific microstructure, taking into account geometry of the pores, and leads to a two-scale model. In [33, 34, 36, 38] the fluid flow and the solid deformation in a viscoelastic porous medium has been modelled using periodic homogenization — a two-scale micro-macro approach based on asymptotic analysis [10, 25, 42, 3, 40].

Here we model the porous structure by using a representative volume element (RVE) describing at the micro-level the behaviour of the fluid in the pores, its action on the pore interfaces, and the viscoelastic deformation of the solid skeleton, cf. [14, 15]. To obtain overall material properties and the so-called macroscopic model, we apply an averaging procedure and rely on a kinematic ansatz which splits the total displacements in the macro- and micro-components.

For the RVE we consider the equilibrium of forces acting on the skeleton which undergoes deformation driven by the macroscopic strain and macroscopic pressure acting on the fluid-solid interface. Equilibrium is ensured by the displacement fluctuation field. Due to the linearity of the problem we see that this field depends linearly on the locally defined overall strains and local pressure. This allows us to introduce characteristic response functions which can be computed by solving boundary value problems defined in the viscoelastic skeleton embedded in the RVE. The upscaling procedure leads to a macroscopic description of the two-phase porous medium, where the force equilibrium and the mass conservation equations involve the effective elasticity tensor, the Biot bulk compressibility modulus and the effective Biot stress tensor which are all expressed in terms of the above mentioned characteristic response functions. The fading memory effects appearing in the macroscopic model are inherited from the solid phase viscoelasticity whereby any such effects associated with fluid flow are neglected. This is a different situation to that studied in [33, 21], where all the memory effects originate in the microflows in the porous structure.

2 Two-scale modelling of the porous structure

We consider two scales: the *problem of interest* is imposed in a domain Ω and coordinates $x \in \Omega$ are related to the *macroscopic* description. The porous structure is described at the *microscopic* scale; it is represented by the RVE (reference volume element) occupying a domain Y. In the periodic homogenization, Y is the periodic cell generating a (locally) periodic material. Here we do not require any periodicity of the medium, as the RVE Y represents just a sample of the material. We recall the essential property that the RVE must be defined to be small enough with respect to (w.r.t) a characteristic size of the macroscopic scale, such as a diameter of Ω, for instance. Keeping in mind this "scale separation", we shall assume that changing the local "microscopic" position y within one RVE does not change the "macroscopic" position x, i.e. x and y are truly independent. It is worth noting that this idea is used in the periodic unfolding method of homogenization, see [10], where any function of x is rewritten into a function of two independent variables, x and y, using the *unfolding*

operator.

The *a priori* decomposition into "macro" and "micro" requires that some boundary conditions (B.C.'s) are supplied for the fluctuating fields on ∂Y. In the periodic homogenization the local fluctuations are periodic; this result is induced by the asymptotic analysis. However, in our treatment such constraints must be imposed ad hoc. It has been surmised in literature, see e.g. [30], that the B.C.'s become "less important" when the RVE becomes larger. Among possible choices we take the simplest one[2] – we assume that the "microscopic" displacement fluctuations vanish on ∂Y.

2.1 Microstructure and modelling assumptions

We consider a decomposition of the microscopic domain: $Y = Y_m \cup Y_c \cup \Gamma$, where $\Gamma = \partial Y_m \cap \partial Y_c$ is the fluid-solid interface, see Fig. 1. Throughout the paper we employ the averages defined for any $K \subset \overline{Y}$, including subdomains and boundaries, as follows:

$$\fint_K (\bullet) = \frac{1}{|Y|} \int_K (\bullet) \, . \tag{1}$$

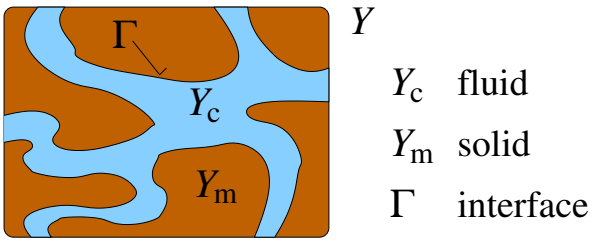

Figure 1: The RVE consisting of solid and fluid occupying domains Y_m and Y_c, respectively. Both Y_m and Y_c are connected independently of the RVE size and of the location.

Scaling and size of the microstructure. Let ε be the characteristic size of the RVE. In the present treatment, we shall assume a kinematic ansatz where the displacement fluctuations are proportional to the scale ε, see (3). Moreover, the following ratio of the measures holds[3]:

$$\frac{|Y|_{3D}}{|\Gamma|_{2D}} \approx \frac{|Y|_{3D}}{|\partial Y|_{2D}} \approx o(\varepsilon) \, , \tag{2}$$

where $|\cdot|_{nD}$ means the measure in nD, $n = 1, 2, 3, \ldots$.

Further by $\boldsymbol{e} = (e_{ij})$ we denote the strain w.r.t. the microscopic coordinates, i.e. using abbreviation $\partial_i^y = \frac{\partial}{\partial y_i}$ for gradients, $e_{ij}(\boldsymbol{v}) = 1/2(\partial_i^y v_j + \partial_j^y v_i)$ for displacements $\boldsymbol{v}(y)$. By default, $\mathrm{div}\boldsymbol{v} = \mathrm{div}_y \boldsymbol{v} = \frac{\partial v_i}{\partial y_i}$, but we shall use also $\mathrm{div}_x \boldsymbol{U} = \frac{\partial U_i}{\partial x_i} = \partial_i^x U_i$.

Kinematic ansatz. Let $\boldsymbol{U}(t, x)$ be the macroscopic displacement at a position $x \in \Omega$ and let us denote by $\boldsymbol{E}(t, x) = (E_{rs}(t, x))$ the local macroscopic (linearized) strain computed using $\boldsymbol{U}$, i.e. $E_{rs} = 1/2(\partial_s^x U_r + \partial_r^x U_s)$, thus, both $\boldsymbol{U}$ and E_{rs} are macroscopic variables

[2]However, all the local problems can be reformulated easily with periodic boundary conditions.

[3]It is worth noting that in the homogenization community, by Y with $|Y|_{3D} = 1$ one referes to the "zoomed" domain, such that εY is the real-sized RVE. However, in the present paper we use $Y := \varepsilon Y$, i.e. $|Y|_{3D} = \varepsilon^3$.

defined in $(t,x) \in [0,T] \times \Omega$. We introduce $\boldsymbol{\Pi}^{rs} = (\Pi_i^{rs})$ with the components defined as $\Pi_i^{rs}(y) = y_s \delta_{ir}$, $y \in Y$, so that the affine transformation $y \mapsto \bar{\boldsymbol{u}} = \boldsymbol{\Pi}^{rs}(y) E_{rs}(t,x)$ represents the displacement field in Y induced by the macroscopic strain; it can be shown easily that $\boldsymbol{e}(\bar{\boldsymbol{u}}) = \boldsymbol{E}$ is the uniform strain in Y, see Remark 1. Alternatively we shall use the abbreviated product $\boldsymbol{\Pi}^{rs} E_{rs} = \boldsymbol{\Pi} : \boldsymbol{E}$.

The displacements at the microscopic scale can be expressed as

$$\begin{aligned} \boldsymbol{u} &= \tilde{\boldsymbol{u}} + \bar{\boldsymbol{u}} + \boldsymbol{U} \\ &= \tilde{\boldsymbol{u}} + \boldsymbol{\Pi} : \boldsymbol{E} + \boldsymbol{U} \ , \end{aligned} \tag{3}$$

where $\tilde{\boldsymbol{u}}(t,x,y)$ are the local fluctuations due to the heterogeneity (porosity), whereby we consider $\tilde{\boldsymbol{u}}(t,x,\cdot) = 0$ on $\partial Y \cap \partial Y_m$. Since $\tilde{\boldsymbol{u}}(t,x,y)$ is not defined in the fluid part, i.e. for $y \in Y_c$, we need to establish an extension from Y_m (the solid) to the entirety of Y; such an extension can be constructed in a number of ways. In what follows we use the same notation for $\tilde{\boldsymbol{u}}(t,x,y)$ when $y \in Y_c$ and $y \in Y_m$.

Remark 1. The idea behind the kinematic ansatz is to split the displacements of points in the RVE into three parts: 1) the translation $\boldsymbol{U}$ of a reference point x defined in the RVE, 2) the relative displacement $\bar{\boldsymbol{u}}$ at $y \in Y$ corresponding to the locally uniform deformation and 3) the displacement fluctuations due to the material heterogeneity. Let us consider a point y defined by its relative coordinates w.r.t. the reference point x. The macroscopic displacement field $\boldsymbol{U}$ is assigned the deformation gradient $\boldsymbol{F} := \boldsymbol{I} + \boldsymbol{E} + \boldsymbol{W}$, where $\boldsymbol{W} = 1/2(\boldsymbol{F} - \boldsymbol{F}^T)$ is the spin tensor. Then $\boldsymbol{y'} := \boldsymbol{F}\boldsymbol{y}$ is the new relative position, so that $\boldsymbol{v} = \boldsymbol{y'} - \boldsymbol{y} = (\boldsymbol{E} + \boldsymbol{W})\boldsymbol{y}$ is the displacement. Now due to the antisymmetry of $\boldsymbol{W}$,

$$\boldsymbol{e}(\boldsymbol{v}) = \boldsymbol{e}(\boldsymbol{E}\boldsymbol{y}) + \boldsymbol{e}(\boldsymbol{W}\boldsymbol{y}) = \boldsymbol{E}.$$

This justifies the use of $\bar{\boldsymbol{u}} = \boldsymbol{E}\boldsymbol{y} = \boldsymbol{\Pi} : \boldsymbol{E}$ instead of $\boldsymbol{v}$ in (3), since the macroscopic spin tensor does not participate in the linearized strain[4].

△

We shall need the set of *admissible displacements*:

$$V_0(Y) = \{ \boldsymbol{v} \in \mathbf{H}^1(Y_m) |\ \boldsymbol{v} = 0 \text{ on } \partial Y,\ \tilde{\boldsymbol{v}} \text{ is a smooth extension of } \boldsymbol{v} \text{ to } Y \} \ . \tag{4}$$

Let us consider the following *assumptions* related to the decomposition (3):

A1) $\|\tilde{\boldsymbol{u}}(t,x\cdot)\|_{\mathbf{L}^2(Y)} \approx o(\varepsilon) |\boldsymbol{U}(t,x)|$ for all $(t,x) \in [0,T] \times \Omega$, thus fluctuations are small when compared to the macroscopic field. On the other hand, $\boldsymbol{e}(\boldsymbol{u}) \approx o(1) \approx \boldsymbol{E}(\boldsymbol{U})$.

A2) The fluctuations vanish[5] on the RVE boundary, i.e. $\tilde{\boldsymbol{u}}(t,x,\cdot) \in V_0(Y)$.

Loading. We assume a quasistatic loading by volume forces $\boldsymbol{f}$ acting in Y_m and by the pore pressure $\bar{p}$ acting on Γ. Further we assume that in the RVE *the pressure is constant* w.r.t. y at any instant t. More precisely, we neglect *a priori* any pressure gradients relevant to the scale ε, cf. [37]. To emphasize this restriction we use the notation $\bar{p}$, instead of just p. However, at the macroscopic scale we allow for pressure nonuniformity, thus $\bar{p} = \bar{p}(t,x)$, which generates the Darcy flow.

[4] In fact, $\boldsymbol{e}(\boldsymbol{v})$ represents the strain w.r.t. the co-rotational coordinate system, which, however, merges with the initial one due to the linearization.

[5] Consistent with the asymptotic homogenization we could use periodic boundary conditions for $\tilde{\boldsymbol{u}}$ on ∂Y. It is well known that the larger RVE is, the smaller is the influence of the boundary conditions on the computed effective properties.

2.2 Model equations at the micro-scale

The model of the porous medium is established using the following equations:

- the equilibrium equation which expresses the balance of virtual work performed by internal and external forces acting on the solid phase when the fluctuatating part of the virtual displacements are considered;
- the mass conservation of the pore fluid in the deforming skeleton;
- the viscoelastic constitutive law for the solid phase;
- the equivalence between the work of averaged stress and the average of the work in the RVE.

Equilibrium equation. The pore pressure $\bar{p}$ presents a macroscopic variable since we assume no local pressure fluctuations. For the solid phase in Y_m pressure $\bar{p}$ acting on Γ presents an external force (traction). The virtual work associated with the test displacements $\delta\boldsymbol{u} := \delta\tilde{\boldsymbol{u}} + \delta\boldsymbol{U} + \boldsymbol{\Pi} : \boldsymbol{E}(\delta\boldsymbol{U})$ is given, as follows,

$$\begin{aligned}\int_{Y_m} \boldsymbol{\sigma} : (\boldsymbol{e}(\delta\tilde{\boldsymbol{u}}) + \boldsymbol{E}(\delta\boldsymbol{U})) = &- \bar{p}\int_{\Gamma} \boldsymbol{n}\cdot(\delta\tilde{\boldsymbol{u}} + \delta\boldsymbol{U} + \boldsymbol{\Pi} : \boldsymbol{E}(\delta\boldsymbol{U}))\mathrm{d}\Gamma \\ &+ \int_{Y_m} \boldsymbol{f}\cdot(\delta\tilde{\boldsymbol{u}} + \delta\boldsymbol{U} + \boldsymbol{\Pi} : \boldsymbol{E}(\delta\boldsymbol{U})) \\ &+ \int_{\partial Y_m\setminus\Gamma} (\boldsymbol{\sigma}\cdot\boldsymbol{n})\cdot(\delta\tilde{\boldsymbol{u}} + \delta\boldsymbol{U} + \boldsymbol{\Pi} : \boldsymbol{E}(\delta\boldsymbol{U}))\mathrm{d}\Gamma\end{aligned} \tag{5}$$

From this equation we can deduce:

1. First let $\delta\tilde{\boldsymbol{u}} = 0$ and also $\boldsymbol{E}(\delta\boldsymbol{U}) = 0$ in Y, whereas $\delta\boldsymbol{U} \neq 0$. In this case (5) yields the overall equilibrium of external forces acting on Y_m.
2. Then let $\delta\tilde{\boldsymbol{u}} = 0$, but $\delta\boldsymbol{E} = \boldsymbol{E}(\delta\boldsymbol{U}) \neq 0$. Obvious calculations lead to the following equation

$$\int_{Y_m} \boldsymbol{\sigma} : \delta\boldsymbol{E} - \bar{p}\int_{Y_c} \boldsymbol{I} : \boldsymbol{E} = \int_{\partial Y} (\boldsymbol{\sigma}\cdot\boldsymbol{n})\cdot\boldsymbol{\Pi} : \delta\boldsymbol{E} + \int_{Y_m} \boldsymbol{f}\cdot\boldsymbol{\Pi} : \delta\boldsymbol{E}\ , \tag{6}$$

where the boundary intergral can be rewritten (note $\delta\boldsymbol{E}$ is constant in y):

$$\int_{\partial Y} (\boldsymbol{\sigma}\cdot\boldsymbol{n})\cdot\boldsymbol{\Pi} = \int_{Y_m\cup Y_c} (\mathrm{div}_y\boldsymbol{\sigma})\cdot\boldsymbol{\Pi} + \int_{Y} \boldsymbol{\sigma}\ . \tag{7}$$

Since $\boldsymbol{\sigma} = -\bar{p}\boldsymbol{I}$ in Y_c, the last term in (7) multiplied by $\delta\boldsymbol{E}$ cancels with the left hand side in (6) and we obtain the condition

$$\int_{Y_m} (\mathrm{div}_y\boldsymbol{\sigma})\cdot\boldsymbol{\Pi} + \int_{Y_m} \boldsymbol{f}\cdot\boldsymbol{\Pi} = 0\ . \tag{8}$$

3. Now we let $\delta \boldsymbol{U}$ vanish, whereas $\delta\tilde{\boldsymbol{u}} \not\equiv 0$. The virtual work principle for the fluctuation test displacements $\boldsymbol{v} = \delta\tilde{\boldsymbol{u}}$ yields

$$\int_{Y_m} \boldsymbol{\sigma}(t) : \boldsymbol{e}(\boldsymbol{v}) = -\bar{p}(t) \int_\Gamma \boldsymbol{n} \cdot \boldsymbol{v} \mathrm{d}\Gamma + \underbrace{\int_{Y_m} \boldsymbol{f} \cdot \boldsymbol{v}}_{\approx 0} , \quad \forall \boldsymbol{v} \in V_0(Y) . \tag{9}$$

From the strong form of the above identity we obtain (8) as an implication. Moreover, in (9), the virtual work done by volume forces $\boldsymbol{f}$ can be neglected in comparison with the work done while macroscopic virtual displacements are considered. This observation is consistent with the asymptotic analysis $\varepsilon \to 0$ in homogenization. The reason for neglecting the virtual work of the volume forces follows from (2) and from the assumption A1. Indeed, while the last intergral in (9) is proportional to ε^{n+1} , the others are $\approx \varepsilon^n$, $n = 2, 3$.

Remark 2. In order to allow for steeper pressure gradients inducing more important flows, we would need to modify interaction between the flow and deformation at the pore level, cf. [11] for acoustic problems, or [8]. In this case pressure fluctuation have the period comparable to the characteristic scale of the microstructure, so that the corresponding interface integral over Γ, see (9), should involve the fluctuating pressure part.

△

Mass conservation. Injection of the fluid – increase in the pore fluid mass $\dot{\zeta}$ – is compensated by increasing the pore size and by the fluid compression (from now on we use $\dot{a} = \frac{\mathrm{d}\, a}{\mathrm{d}\, t}$ to denote the time derivative), thus

$$-\int_{\partial Y_c} \boldsymbol{z} \cdot \boldsymbol{n}^c \mathrm{d}\Gamma = |Y_c|\dot{\zeta} = \int_{\partial Y_c} \dot{\boldsymbol{u}} \cdot \boldsymbol{n}^c \mathrm{d}\Gamma + \gamma\dot{\bar{p}}|Y_c| , \tag{10}$$

where $\gamma \geq 0$ is the fluid compressibility, $\boldsymbol{z} = \boldsymbol{v}^f - \dot{\boldsymbol{u}}$ is the relative velocity of the fluid and the normal vector $\boldsymbol{n}^c$ is oriented outwards to Y_c. Due to the decomposition of ∂Y, and using the extension of $\boldsymbol{u}$ to the entire Y (note that only the part $\tilde{\boldsymbol{u}}$ must be extended, whereby $\tilde{\boldsymbol{u}} = 0$ must hold on ∂Y, see (3)), we have

$$\begin{aligned} \int_{\partial Y_c} \dot{\boldsymbol{u}} \cdot \boldsymbol{n}^c \mathrm{d}\Gamma &= \int_{\partial Y} \dot{\boldsymbol{u}} \cdot \boldsymbol{n}^c \mathrm{d}\Gamma + \int_\Gamma \dot{\boldsymbol{u}} \cdot \boldsymbol{n}^c \mathrm{d}\Gamma - \int_{\partial Y_m \cap \partial Y} \dot{\boldsymbol{u}} \cdot \boldsymbol{n}^m \mathrm{d}\Gamma \\ &= \int_{\partial Y} \dot{\boldsymbol{u}} \cdot \boldsymbol{n} \mathrm{d}\Gamma - \int_{\partial Y_m} \dot{\boldsymbol{u}} \cdot \boldsymbol{n}^m \mathrm{d}\Gamma . \end{aligned} \tag{11}$$

Further we apply the displacement decomposition (9), so that on denoting $\bar{\boldsymbol{u}} := \boldsymbol{E} : \boldsymbol{\Pi}$, (10) and (11) yield

$$\int_Y \mathrm{div}\dot{\tilde{\boldsymbol{u}}} + \int_{\partial Y} \dot{\tilde{\boldsymbol{u}}} \cdot \boldsymbol{n} \mathrm{d}\Gamma - \int_{Y_m} \mathrm{div}(\dot{\bar{\boldsymbol{u}}} + \dot{\tilde{\boldsymbol{u}}}) + \gamma\dot{p}|Y_c| = \dot{\zeta}|Y_c| . \tag{12}$$

We recall $\tilde{\boldsymbol{u}} = 0$ on ∂Y, therefore, the 2nd integral vanishes so that the mass conservation (12) attains the following form:

$$\begin{aligned} \phi\delta_{rs}\dot{E}_{rs} - \fint_{Y_m} \mathrm{div}_y \dot{\tilde{\boldsymbol{u}}} + \gamma\phi\dot{p} &= \phi\dot{\zeta} , \\ \text{or} \quad \phi \mathrm{div}_x \dot{\boldsymbol{U}} - \fint_{Y_m} \mathrm{div}_y \dot{\tilde{\boldsymbol{u}}} + \gamma\phi\dot{p} &= \phi\dot{\zeta} , \end{aligned} \tag{13}$$

Where we introduced the volume fraction $\phi = \frac{|Y_c|}{|Y|}$.

Constitutive viscoelastic law. The solid phase stress $\boldsymbol{\sigma} = (\sigma_{ij})$ is defined at $(x, y) \in \Omega \times Y_m$, as follows

$$\begin{aligned} \boldsymbol{\sigma}(t) &= \mathbb{D} \int_0^t \varphi(t-s) \frac{\mathrm{d}}{\mathrm{d}\, s} \boldsymbol{e}(\boldsymbol{u}(s)) \mathrm{d}s \ , \quad y \in Y_m \ , \\ \varphi(t) &= \varphi_0 + \varphi_1 \exp\{-t/\tau\} \ , \quad \varphi(0) = 1 \ , \end{aligned} \tag{14}$$

where $\mathbb{D} = (D_{ijkl})$ is the usual elasticity tensor. In general φ_0, φ_1 and $\mathbb{D}$ can be functions of both the micro- and macro-coordinates (x, y).

Using (14) we express the stress as a piecewise defined function in the two phases (note $\boldsymbol{I} = (\delta_{ij})$):

$$\boldsymbol{\sigma}(t, x, y) := \begin{cases} \mathbb{D} \int_0^t \varphi(t-s) \frac{\mathrm{d}}{\mathrm{d}\, s} \boldsymbol{e}(\boldsymbol{u}(s)) \mathrm{d}s & \text{for } y \in Y_m \ , \\ -\bar{p}(t, x) \boldsymbol{I} & \text{for } y \in Y_c \ . \end{cases} \tag{15}$$

Since we assume quasistatic events only which are characterized by extremely slow flows in the porous structure, we can neglect the dissipative part of the stress tensor in the fluid, thus, the fluid viscosity effects are disregarded at the microscopic level. For the same reason we neglect possible pressure fluctuations at the microscopic scale. To justify these simplifications, in Remark 4, see Section 4, we put some numbers illustrating relevance of the stress defined in (15) for practical simulations.

The averaged stress and the virtual work of the stress. We shall use the equivalence of the microscopic virtual work and its macroscopic interpretation: $\boldsymbol{S} = (S_{ij})$ is the equivalent macroscopic stress if

$$\fint_Y \big(\boldsymbol{\sigma} : \boldsymbol{e}(\delta \boldsymbol{u})\big) = \boldsymbol{S} : \delta \boldsymbol{E} = \fint_Y \boldsymbol{\sigma} : \fint_Y \boldsymbol{e}(\delta \boldsymbol{u}) \ . \tag{16}$$

This statement is often refered to as *Hill's lemma*, see [22, 23, 29]. $\boldsymbol{S}$ is computed as the stress average over the RVE and $\delta \boldsymbol{E}$ is the strain average, since using (3)

$$\fint_Y \boldsymbol{e}(\delta \boldsymbol{u}) = \fint_Y \big(\boldsymbol{e}(\delta \tilde{\boldsymbol{u}}) + \delta \boldsymbol{E}\big) = \delta \boldsymbol{E} \ , \tag{17}$$

where we used $\int_Y \boldsymbol{e}(\delta \tilde{\boldsymbol{u}}) = \int_{\partial Y} \boldsymbol{n} \otimes \tilde{\boldsymbol{u}} = 0$ and $e_{ij}(\boldsymbol{\Pi}^{kl}) = \delta_{ik}\delta_{jl}$. The equivalence (16) is trivial whenever the local virtual displacements are generated by the homogeneous macroscopic virtual strain $\delta \boldsymbol{E} = (\delta E_{ij})$, so that defining $\delta_E \boldsymbol{v} := \boldsymbol{\Pi}^{rs}(y) \delta E_{rs}$, we have that $\boldsymbol{e}(\delta_E \boldsymbol{v}) = \delta \boldsymbol{E}$ and consequently

$$\fint_Y \boldsymbol{\sigma} : \boldsymbol{e}(\delta_E \boldsymbol{v}) = \boldsymbol{S} : \delta \boldsymbol{E} \ . \tag{18}$$

Hence, the equivalent macroscopic stress is just the average of $\boldsymbol{\sigma}$ computed over the whole of Y,

$$\boldsymbol{S} := \fint_Y \boldsymbol{\sigma} = \fint_{Y_m} \boldsymbol{\sigma} - \phi \bar{p} \boldsymbol{I} \ . \tag{19}$$

The statement of the equivalence lemma (16) is an easy consequence of the local equilibrium (9), since then we have that

$$\int_Y \boldsymbol{\sigma} : \boldsymbol{e}(\delta \boldsymbol{u}) = \int_Y (\boldsymbol{\sigma} : \boldsymbol{e}(\delta \tilde{\boldsymbol{u}})) + \int_Y \boldsymbol{\sigma} : \delta \boldsymbol{E} = \boldsymbol{S} : \delta \boldsymbol{E} \ . \tag{20}$$

Two-scale model – summary. Let us now recall that the porous medium is represented by the RVE Y with the microstructure given by the pore geometry Y_c and by inhomogeneities of $\mathbb{D}$ defined in Y_m, whereas the relaxation function $\varphi(t)$ and the fluid compressibility γ are constant in space. Deformations are described by two-scale displacement fields $(\boldsymbol{u}, \boldsymbol{U})$ which satisfy (5), (9), (13) and (15). The "fluid equation" requires some inital conditions: for simplicity we shall consider the *unloaded inital state*, i.e. $\boldsymbol{E}(t \leq 0) = 0, \tilde{\boldsymbol{u}}(t \leq 0) = 0, \zeta(t \leq 0) = 0$ and consistently $\bar{p}(t \leq 0) = 0$.

In Section 5 we describe a more general situation, where the initial steady state is considered.

3 Micro-macro decomposition of the response

We use the Laplace transformation: $\mathcal{L}\{f(t)\} = \underset{*}{f}(\lambda)$, where λ is the Laplace variable. Let $\Phi(\lambda) = \mathcal{L}\{\varphi(t)\}$ be the transformed relaxation function and introduce the transformed creep function: $\Psi(\lambda) = (\lambda^2\Phi)^{-1}$, so that $\psi(t) = \mathcal{L}^{-1}\{\Psi(\lambda)\}$, with $\psi(0) = 1$; the last statement can be verified easily upon applying $\mathcal{L}^{-1}\{\}$ to the equation $\lambda\Phi\Psi = 1/\lambda$, recalling $\varphi(0) = 1$. The viscoelastic constitutive law (in the solid) is transformed as follows:

$$\begin{aligned} \text{relaxation form:} \quad & \underset{*}{\boldsymbol{\sigma}} = \mathbb{D}\Phi(\lambda)\lambda\underset{*}{\boldsymbol{e}} \,, \\ \text{creep form:} \quad & \underset{*}{\boldsymbol{e}} = \mathbb{D}^{-1}\Psi(\lambda)\lambda\underset{*}{\boldsymbol{\sigma}} \,. \end{aligned} \tag{21}$$

3.1 Homogenized equations under the Laplace transformation of time

The Laplace transformation of the kinematic ansatz (3) yields $\underset{*}{\boldsymbol{u}} = \underset{*}{\tilde{\boldsymbol{u}}} + \boldsymbol{\Pi}^{rs}\underset{*}{E}_{rs} + \underset{*}{\boldsymbol{U}}$, where obviously $\underset{*}{E}_{rs} = E_{rs}(\underset{*}{\boldsymbol{U}})$. Since in the local equilibrium equation (9) $\bar{p}$ and E_{rs} are the macroscopic variables, i.e. independent of y, we define the following decomposition:

$$\underset{*}{\tilde{\boldsymbol{u}}} = \lambda\underset{*}{\boldsymbol{w}}^{rs}\underset{*}{E}_{rs} - \lambda\underset{*}{\bar{p}}\,\underset{*}{\boldsymbol{w}}^{P} \,. \tag{22}$$

According to (15),

$$\begin{aligned} \underset{*}{\boldsymbol{\sigma}} &= \Phi(\lambda)\mathbb{D} : \lambda\boldsymbol{e}(\lambda\underset{*}{\boldsymbol{w}}^{rs}\underset{*}{E}_{rs} + \boldsymbol{\Pi}^{rs}\underset{*}{E}_{rs} - \lambda\underset{*}{\bar{p}}\,\underset{*}{\boldsymbol{w}}^{P}) \,, \\ \underset{*}{\boldsymbol{S}} &= \fint_{Y_m} \underset{*}{\boldsymbol{\sigma}} - \phi\boldsymbol{I}\underset{*}{\bar{p}} \,. \end{aligned} \tag{23}$$

The macroscopic stress (23) can now be expressed in terms of the homogenized (effective) coefficients

$$\underset{*}{S}_{ij} = \lambda^2\Phi(\lambda)\underset{*}{A}_{ijkl}\underset{*}{E}_{kl} - \left(\lambda^2\Phi(\lambda)\underset{*}{\beta'}_{ij} + \delta_{ij}\phi\right)\underset{*}{\bar{p}} \,, \tag{24}$$

where

$$\begin{aligned} \underset{*}{A}_{ijkl} &= \fint_{Y_m} D_{ijrs}e_{rs}(\underset{*}{\boldsymbol{w}}^{kl} + \frac{1}{\lambda}\boldsymbol{\Pi}^{kl}) \\ &= \fint_{Y_m} \mathbb{D}\,\boldsymbol{e}(\underset{*}{\boldsymbol{w}}^{kl} + \frac{1}{\lambda}\boldsymbol{\Pi}^{kl}) : \boldsymbol{e}(\boldsymbol{\Pi}^{ij}) \,, \\ \underset{*}{\beta'}_{ij} &= \fint_{Y_m} D_{ijkl}e_{kl}(\underset{*}{\boldsymbol{w}}^{P}) = \fint_{Y_m} \mathbb{D}\,\boldsymbol{e}(\underset{*}{\boldsymbol{w}}^{P}) : \boldsymbol{e}(\boldsymbol{\Pi}^{ij}) \,. \end{aligned} \tag{25}$$

Due to the zero initial conditions, by the Laplace-transformation of $(13)_1$ and using (22) we obtain

$$\begin{aligned}
&\phi\delta_{rs}\lambda \underset{*}{E}_{rs} - \lambda \fint_{Y_m} \mathrm{div}_y \tilde{\underset{*}{\boldsymbol{u}}} + \lambda\gamma\phi \underset{*}{p} = \lambda\phi \underset{*}{\zeta} \ , \\
&\lambda^2 \left(\frac{\phi\delta_{rs}}{\lambda} - \fint_{Y_m} \mathrm{div}_y \underset{*}{\boldsymbol{w}}^{rs} \right) \underset{*}{E}_{rs} + \lambda^2 \left(\frac{\phi\gamma}{\lambda} + \fint_{Y_m} \mathrm{div}_y \underset{*}{\boldsymbol{w}}^{P} \right) \underset{*}{\bar{p}} = \phi\lambda \underset{*}{\zeta} \ ,
\end{aligned} \tag{26}$$

where the initial fluctuations vanish by the assumption $\tilde{\boldsymbol{u}}(0) = 0$. We define

$$\underset{*}{\beta}_{rs} = -\fint_{Y_m} \mathrm{div}_y \underset{*}{\boldsymbol{w}}^{rs} = -\fint_{\Gamma} \underset{*}{\boldsymbol{w}}^{rs} \cdot \boldsymbol{n} \mathrm{d}\Gamma \ , \qquad \underset{*}{\mu} = \fint_{Y_m} \mathrm{div}_y \underset{*}{\boldsymbol{w}}^{P} \ , \tag{27}$$

so that (26) yields

$$(\phi\delta_{ij} + \lambda \underset{*}{\beta}_{ij})\lambda \underset{*}{E}_{ij} + (\phi\gamma + \lambda \underset{*}{\mu})\lambda \underset{*}{p} = \lambda\phi \underset{*}{\zeta} \ . \tag{28}$$

As the next step we introduce local microscopic problems to compute the characteristic fluctuation displacements and express the homogenized (effective) coefficients in the time domain, after applying the inverse Laplace transformation.

3.2 Equilibrium equation – local problems

On transforming (9) with $\boldsymbol{\sigma}$ being substituted from (14), i.e. using $(23)_1$, we get

$$\int_{Y_m} \lambda\Phi(\lambda) \mathbb{D}\boldsymbol{e} \left(\lambda \underset{*}{\boldsymbol{w}}^{rs} \underset{*}{E}_{rs} + \boldsymbol{\Pi}^{rs} \underset{*}{E}_{rs} - \lambda \underset{*}{\bar{p}} \underset{*}{\boldsymbol{w}}^{P} \right) : \boldsymbol{e}(\boldsymbol{v}) = -\underset{*}{\bar{p}} \int_{\Gamma} \boldsymbol{n} \cdot \boldsymbol{v} \mathrm{d}\Gamma \ , \tag{29}$$

$\forall \boldsymbol{v} \in V_0(Y)$, see definition (4). We shall use the following bilinear form:

$$a_Y^m(\boldsymbol{w}, \boldsymbol{v}) = \int_{Y_m} \mathbb{D}\boldsymbol{e}(\boldsymbol{w}) : \boldsymbol{e}(\boldsymbol{v}) \ . \tag{30}$$

Note that due to positive-definitness of $\mathbb{D}$, $a_Y^m(\cdot, \cdot)$ induces an energy norm on the nonempty space $V_0(Y_m)$, the restriction of $V_0(Y)$ to functions defined only in Y_m with zero trace on $\partial Y \cap \partial Y_m$.

Due to linearity we may define the following local problems:

1. Compute $\underset{*}{\boldsymbol{w}}^{rs} \in V_0(Y)$ such that

$$a_Y^m \left(\underset{*}{\boldsymbol{w}}^{rs} + \frac{1}{\lambda} \boldsymbol{\Pi}^{rs}, \boldsymbol{v} \right) = 0 \quad \forall \boldsymbol{v} \in V_0(Y) \ . \tag{31}$$

2. Compute $\underset{*}{\boldsymbol{w}}^{P} \in V_0(Y)$ such that

$$\lambda\Phi a_Y^m \left(\underset{*}{\boldsymbol{w}}^{P}, \boldsymbol{v} \right) = \frac{1}{\lambda} \int_{\Gamma} \boldsymbol{n} \cdot \boldsymbol{v} \mathrm{d}\Gamma \quad \forall \boldsymbol{v} \in V_0(Y) \ . \tag{32}$$

Obviously, returning back in the time domain, (31) yields

$$a_Y^m\left(\boldsymbol{w}^{rs}+\boldsymbol{\Pi}^{rs},\,\boldsymbol{v}\right)=0\quad\forall\boldsymbol{v}\in V_0(Y)\;, \tag{33}$$

so that $\boldsymbol{w}^{rs}$ is constant in time.

In contrast, $\boldsymbol{w}^P(t,\cdot)$ solves an evolutionary problem which can be presented in the following form (note $\varphi(0)=1$)

$$\begin{gathered}\int_0^t a_Y^m\left(\boldsymbol{w}^P(s),\,\boldsymbol{v}\right)\dot{\varphi}(t-s)\mathrm{d}s+a_Y^m\left(\boldsymbol{w}^P(t),\,\boldsymbol{v}\right)=a_Y^m\left(\boldsymbol{w}^P(0),\,\boldsymbol{v}\right)\;,\\ \text{with}\quad a_Y^m\left(\boldsymbol{w}^P(0),\,\boldsymbol{v}\right)=\int_\Gamma\boldsymbol{n}\cdot\boldsymbol{v}\mathrm{d}\Gamma\;,\quad\forall\boldsymbol{v}\in V_0(Y)\;.\end{gathered} \tag{34}$$

It is worth noting that in problems (31)-(34) we can replace $V_0(Y)$ by its restriction $V_0(Y_m)$. Since $a_Y^m(\cdot,\cdot)$ is coercive on $V_0(Y_m)$, as discussed above, in the Laplace-transformed domain, $(34)_1$ is equivalent with

$$\underset{*}{\boldsymbol{w}}{}^P=\frac{1}{\lambda^2\Phi}\boldsymbol{w}^P(0)=\Psi\,\boldsymbol{w}^P(0)\;, \tag{35}$$

so that evolution of $\boldsymbol{w}^P$ is driven by the creep response function.

4 Effective constitutive laws in time domain

First we establish the homogenized coefficients β_{ij} and μ in the time domain. Due to (see (27))

$$\underset{*}{\mu}=\fint_\Gamma\boldsymbol{n}\cdot\underset{*}{\boldsymbol{w}}{}^P\mathrm{d}\Gamma=\Psi\fint_\Gamma\boldsymbol{n}\cdot\boldsymbol{w}^P(0)\mathrm{d}\Gamma\;, \tag{36}$$

and recalling $\psi(t)=\mathcal{L}^{-1}\{\Psi(\lambda)\}$ we have,

$$\mu(t)=\hat{\mu}\psi(t)\;,\qquad\text{where}\qquad\hat{\mu}=\fint_\Gamma\boldsymbol{n}\cdot\boldsymbol{w}^P(0)\mathrm{d}\Gamma \tag{37}$$

is the skeleton compressibility; we remark that $\hat{\mu}>0$ due to $(34)_2$.

We can prove $\lambda\Phi\underset{*}{\beta'}_{ij}=\underset{*}{\beta}_{ij}$, see $(25)_2$ and (27). From (31) and (32)

$$\begin{gathered}\underset{*}{\beta'}_{rs}=\int_{Y_m}\mathbb{D}\boldsymbol{e}(\underset{*}{\boldsymbol{w}}{}^P):\boldsymbol{e}(\boldsymbol{\Pi}^{rs})=-\lambda\int_{Y_m}\mathbb{D}\boldsymbol{e}(\underset{*}{\boldsymbol{w}}{}^P):\boldsymbol{e}(\underset{*}{\boldsymbol{w}}{}^{rs})=-\frac{1}{\lambda\Phi}\int_\Gamma\boldsymbol{n}\cdot\underset{*}{\boldsymbol{w}}{}^{rs}\mathrm{d}\Gamma\;,\\ \Rightarrow\quad\lambda\Phi\underset{*}{\beta'}_{ij}=-\fint_\Gamma\boldsymbol{n}\cdot\underset{*}{\boldsymbol{w}}{}^{ij}\mathrm{d}\Gamma=-\fint_{Y_m}\mathrm{div}_y\underset{*}{\boldsymbol{w}}{}^{ij}=\underset{*}{\beta}_{ij}\;,\end{gathered} \tag{38}$$

where we used $\underset{*}{\boldsymbol{w}}{}^{ij}\in V_0(Y)$. Since $\boldsymbol{w}^{ij}$ is time independent, A_{ijkl} and β_{ij} are constant in time as well. Hence

$$\underset{*}{A}_{ijkl}=\frac{1}{\lambda}A_{ijkl}\;,\quad\underset{*}{\beta}_{ij}=\frac{1}{\lambda}\beta_{ij}\;, \tag{39}$$

elasticity	$\mathbb{A} = (A_{ijkl})$	$A_{ijkl} = A_{klij} = A_{jikl}$	$\mathbb{A} \succ 0$
Biot's stress coefficients	$\boldsymbol{\beta} + \phi \boldsymbol{I} = (\beta_{ij} + \phi\delta_{ij})$	$\beta_{ij} = \beta_{ji}$	
skeleton compressibility	$\hat{\mu}$		$\hat{\mu} > 0$

Table 1: Effective poroelastic coefficients — important properties.

and we get the following formulae, where the symmetric expression for the effective elasticity tensor A_{ijkl} is obtained using (33):

$$\begin{aligned} A_{ijkl} &= a_Y^m \left(\boldsymbol{w}^{kl} + \boldsymbol{\Pi}^{kl}, \boldsymbol{\Pi}^{ij} \right) = a_Y^m \left(\boldsymbol{w}^{kl} + \boldsymbol{\Pi}^{kl}, \boldsymbol{w}^{ij} + \boldsymbol{\Pi}^{ij} \right) , \\ \beta_{ij} &= - \fint_{Y_m} \mathrm{div}_y \boldsymbol{w}^{ij} = - \fint_{\Gamma} \boldsymbol{w}^{ij} \cdot \boldsymbol{n} \mathrm{d}\Gamma . \end{aligned} \tag{40}$$

Obviously, due to the microscopic problem, the tensor A_{ijkl} is symmetric and positive definite (the major and minor symmetries are inherited from D_{ijkl}). The poroelastic (Biot's) stress coefficient β_{ij} is symmetric and we note that it describes the skeleton shrinkage, i.e. the volume change induced by the macroscopic deformation. All the effective coefficients of poroelasticity are listed in Tab. 1.

4.1 Stress

Using (39) and $(38)_2$, we can rewrite (24):

$$\underset{*}{S}_{ij} = \lambda \Phi A_{ijkl} \underset{*}{E}_{kl} - (\beta_{ij} + \phi\delta_{ij}) \underset{*}{\bar{p}} \tag{41}$$

By the inverse Laplace transformation of (24) we obtain the effective stress which obeys the poro-viscoelastic constitutive law

$$S_{ij}(t) = A_{ijkl} \int_0^t \varphi(t-s) \frac{\mathrm{d}}{\mathrm{d}\, s} E_{kl}(s) \mathrm{d}s - (\beta_{ij} + \phi\delta_{ij}) \bar{p}(t) . \tag{42}$$

4.2 Mass conservation

Using (27),(36) and (39), from (28) we obtain

$$(\phi\delta_{ij} + \beta_{ij}) \lambda \underset{*}{E}_{ij} + (\phi\gamma + \lambda\hat{\mu}\Psi) \lambda \underset{*}{p} = \lambda \underset{*}{\phi\zeta} . \tag{43}$$

Hence, the inverse Laplace transformation yields

$$(\phi\delta_{kl} + \beta_{kl}) \dot{E}_{kl}(t) + \phi\gamma \dot{\bar{p}}(t) + \hat{\mu} \int_0^t \dot{\psi}(t-s) \frac{\mathrm{d}}{\mathrm{d}\, s} \bar{p}(s) \mathrm{d}s + \hat{\mu} \dot{\bar{p}} = \phi \dot{\zeta} . \tag{44}$$

We recall that $\phi\dot{\zeta}$ is the fluid content increase at a given "macroscopic" point which can be expressed by the Darcy flow at the macroscopic scale, thus

$$\phi \dot{\zeta} = -\mathrm{div}_x \boldsymbol{W} , \quad \boldsymbol{W} = -\boldsymbol{K} \nabla_x \bar{p} , \tag{45}$$

where $\boldsymbol{W}$ is now the seepage velocity (not to be confused with the spin tensor used in Section 2.1). Above $\boldsymbol{K} = (K_{ij})$ is the hydraulic permeability which can be computed for a given geometry of the porosity represented by domain Y_c, see e.g. [2, 25]. Here the permeability is introduced ad hoc, since we disregarded fluid flow effects at the microscopic level during the model upscaling, as described in the preceding sections.

4.3 Poro-viscoelastic constitutive law

We can now state the main result of the paper. Let us assume that:

- a given microscale structure consists of the fluid and solid phases, the solid skeleton forms a connected domain, as well as the fluid phase (Such situation is natural in 3D, but impossible in 2D, although a meaningful problem can be formulated in 2D, see Remark 3);
- the viscoelastic response in the solid phase is defined in $(15)_1$;
- the static pressure is evenly distributed at the microscopic scale, i.e. pressure gradients at the microscopic scale are negligible, as discused above in Remark 2. No viscous effects related to the fluid flow are considered when dealing with the fluid-solid interaction at the pore level and the stress is defined by $(15)_2$.

Recalling the zero initial conditions, i.e. $\boldsymbol{E}(t=0)=0$, the stress in the upscaled poro-viscoelasticity continuum is

$$\begin{aligned} S_{ij} &= A_{ijkl}\int_0^t \varphi(t-s)\frac{\mathrm{d}}{\mathrm{d}\,s}E_{kl}(s)\mathrm{d}s - (\beta_{ij}+\phi\delta_{ij})\bar{p} \\ &= A_{ijkl}E_{kl}(t) + A_{ijkl}\int_0^t \dot{\varphi}(t-s)E_{kl}(s)\mathrm{d}s - (\beta_{ij}+\phi\delta_{ij})\bar{p}\,, \end{aligned} \tag{46}$$

and the local pressure $\bar{p}$ must satisfy the macroscopic fluid mass conservation

$$\nabla\cdot\boldsymbol{K}\nabla\bar{p} = (\phi\delta_{kl}+\beta_{kl})\,\dot{E}_{kl} + (\phi\gamma+\hat{\mu})\dot{\bar{p}} + \hat{\mu}\int_0^t \dot{\psi}(t-s)\frac{\mathrm{d}}{\mathrm{d}\,s}\bar{p}(s)\mathrm{d}s\,, \tag{47}$$

where $\dot{\varphi}(t)=\frac{\mathrm{d}}{\mathrm{d}\,t}\varphi(t)$. We used (45) to replace the term $\phi\dot{\zeta}$.

Let us note that $\hat{\mu}>0$, therefore, even for the incompressible fluid, when $\gamma=0$, the mathematical structure of the upscaled problem does not change. For the relaxation function stated in (14) we have $\psi(t)=\psi_0-\psi_1\exp\{-(\varphi_0/\tau)t\}$ with $\psi_0=1/\varphi_0$ and $\psi_1=\varphi_1/\varphi_0$, $\varphi_0>0$, so that the memory term involving the kernel $\dot{\psi}$ reads as

$$\hat{\mu}\int_0^t \dot{\psi}(t-s)\frac{\mathrm{d}}{\mathrm{d}\,s}\bar{p}(s)\mathrm{d}s = \hat{\mu}\frac{\varphi_1}{\tau}\int_0^t e^{-(t-s)/\tau}\frac{\mathrm{d}}{\mathrm{d}\,s}\bar{p}(s)\mathrm{d}s\,.$$

Remark 3. In many cases, problems motivated by a real situation require to be formulated in 3D, as in 2D some important topological and geometrical assumptions cannot be satisfied. In our case, 2D problems can be considered, although the RVE subdomains Y_m and Y_c cannot generate simultaneously connected domains in 2D. Assume that $Y_c\subset Y$ is an inclusion, then all the effective constants $\mathbb{A}$, $\boldsymbol{\beta}$ and $\hat{\mu}$ are well defined, since problems (31)-(34) are well posed. However, there is no fluid flow outside the inclusions, i.e. $\dot{\zeta}=0$ and, thus, the permeability is zero in (47).

△

To conclude this section we present a problem formulation for our upscaled poro-viscoelastic model. For this we need to set boundary conditions. In general, we may consider the following split of boundary $\partial\Omega$ ("up to the zero measure manifolds"):

$$\begin{aligned} &\partial\Omega = \partial_\sigma\Omega\cup\partial_u\Omega\,, \quad \partial_\sigma\Omega\cap\partial_u\Omega=\emptyset\,, \\ &\partial\Omega = \partial_w\Omega\cup\partial_p\Omega\,, \quad \partial_w\Omega\cap\partial_p\Omega=\emptyset\,. \end{aligned} \tag{48}$$

The following mixed boundary conditions can be prescribed to simulate a very general consolidation problem:

$$\begin{aligned} \boldsymbol{U} &= \boldsymbol{U}^{BC} \quad \text{on } \partial_u\Omega\,, \\ \boldsymbol{n}\cdot\boldsymbol{S} &= \boldsymbol{g}^{BC} \quad \text{on } \partial_\sigma\Omega\,, \\ p &= p^{BC} \quad \text{on } \partial_p\Omega\,, \\ \boldsymbol{n}\cdot\boldsymbol{W} &= w_n^{BC} \quad \text{on } \partial_w\Omega\,, \end{aligned} \tag{49}$$

where $\boldsymbol{n}=(n_i)$ is the unit normal outward to Ω and by superscript $\square^{BC}$ we denote prescribed quantities on subsets of $\partial\Omega$.

Assuming the zero initial conditions, i.e. $\boldsymbol{U}(x,0)=0$ and $p(x,0)=0$ for $x\in\Omega$ and the boundary condition (49), the couple $(\boldsymbol{U}(x,t),p(x,t))$ satisfies the following system of equations for $(x,t)\in\Omega\times]0,T[$

$$\begin{aligned} \nabla\cdot\left(\mathbb{A}\int_0^t\varphi(t-s)\boldsymbol{E}(\frac{\mathrm{d}}{\mathrm{d}\,s}\boldsymbol{U}(s))\mathrm{d}s-(\phi\boldsymbol{I}+\boldsymbol{\beta})p\right)&=\boldsymbol{f}\,,\\ (\phi\boldsymbol{I}+\boldsymbol{\beta}):\boldsymbol{E}(\frac{\mathrm{d}}{\mathrm{d}\,t}\boldsymbol{U}(t))-\nabla\cdot\boldsymbol{K}\nabla\bar{p}+(\phi\gamma+\hat{\mu})\dot{p}+\hat{\mu}\int_0^t\dot{\psi}(t-s)\frac{\mathrm{d}}{\mathrm{d}\,s}p(s)\mathrm{d}s&=0\,. \end{aligned} \tag{50}$$

Remark 4. In this remark we demonstrate smallness of the fluid viscosity effects and pressure fluctuations at the microscopic level for highly pervious structures when small pressure gradients are allowed. For instance, we may consider porous structure formed by parallel tubes of the diameter $d=10^{-4}$ [m] with porosity $\phi=0.5$ saturated by water, the dynamic viscosity $\eta_w=10^{-3}$ [Pa.s]. We allow for pressure gradients $|\nabla_x p|=100$ [Pa/m], which means that the pressure variation at the microscopic scale $\ell\approx 1$ [mm] is about 0.1 [Pa]. Simple calculations based on the Hagen–Poiseuille equation yield the permeability $K=1.5625\cdot10^{-7}$ [m^2/(Pa.s)], the average fluid velocity $\bar{v}=1.5625\cdot10^{-5}$ [m/s] ($\bar{v}=0.05625$ [m/hour]) and the wall shear stress at the solid-fluid interface $\sigma_{ws}=2.5\cdot10^{-3}$ [Pa]. Thus, the wall shear stresses and pressure fluctuations are really negligible in the context of stresses induced in the solid and fluid, ranging 10 to 100 [kPa]. Also the fluid flow is slow, so that all inertia effects can be neglected.

Obviously, the above low flow rates and small viscosity have negligible influence on the fluid-structure interaction as the consequences of relatively large permeability and low pressure gradients; to ensure the latter factor, the loading by external forces must be very slow and the relaxation time of the viscoelastic solid should be large enough.

△

5 Generalization for non-zero initial conditions

First it should be emphasized that the initial conditions should reflect an admissible physical situation. A reasonable assumption is that the initial conditions at $t=0$ correspond to a *steady state* equilibrium $\boldsymbol{q}^\flat:=(\boldsymbol{U}^\flat,p^\flat)$ for $t\le 0$. Due to linearity we may easily consider

$$\boldsymbol{q}(t)=\boldsymbol{q}^\flat+\boldsymbol{q}^\clubsuit(t)\quad\text{ with }\quad\boldsymbol{q}^\clubsuit(t=0)=0\,. \tag{51}$$

We shall now derive equations governing the steady state solution $\boldsymbol{q}^\flat$ and for this we use the fading memory property of the convolution kernels φ and ψ. Let T^δ_φ and T^δ_ψ be such that

$$\Big|\int_0^\infty \dot\varphi(s)\mathrm{d}s - \int_0^{T^\delta_\varphi} \dot\varphi(s)\mathrm{d}s\Big| \le \delta\ , \quad \& \quad \Big|\int_0^\infty \dot\psi(s)\mathrm{d}s - \int_0^{T^\delta_\psi} \dot\psi(s)\mathrm{d}s\Big| \le \delta\ . \tag{52}$$

For any error $\delta \to 0$ we can find appropriate times T^δ_φ and T^δ_ψ. Let $\bar T = \max\{T^\delta_\varphi, T^\delta_\psi\}$. Further we assume that a steady state is attained at $\bar t < t - \bar T$ by an evolution from the "zero initial state", governed by (46),(47). Obviously, for $t >> \bar t + \bar T$ we have

$$\psi(t-\bar t) \approx \psi_0\ , \quad \varphi(t-\bar t) \approx \varphi_0\ . \tag{53}$$

5.1 Steady state equations

The following equations derived from (46),(47) hold up to an error $\approx \delta$.

Equilibrium equation. For simplicity, let us consider $\boldsymbol{U}^\flat$ given on $\partial\Omega$, recalling Ω is the "macroscopic domain" with boundary $\partial\Omega$. The equlibrium equation reads (in the weak sense in the dual to $\mathbf{H}^1_0(\Omega)$)

$$-\nabla\cdot\boldsymbol{S}(\boldsymbol{q}^\flat) = \boldsymbol{f} \quad \text{ in } \Omega\ . \tag{54}$$

Using property (52), from (46) we deduce for $E_{kl}(-\infty) = 0$ and $t > \bar t + \bar T$ (neglecting $\int_{-\infty}^{t-\bar T} \dot\varphi(t-s)E_{kl}(s)\mathrm{d}s$) the following stress

$$\begin{aligned} S_{ij}(t) &\approx A_{ijkl}E^\flat_{kl} + A_{ijkl}E^\flat_{kl}\int_{t-\bar T}^t \dot\varphi(t-s)\mathrm{d}s - (\beta_{ij}+\phi\delta_{ij})p^\flat \\ &= \varphi(t-\bar t)A_{ijkl}E^\flat_{kl} - (\beta_{ij}+\phi\delta_{ij})p^\flat \\ &\approx \varphi_0 A_{ijkl}E^\flat_{kl} - (\beta_{ij}+\phi\delta_{ij})p^\flat =: S^\flat_{ij}(\boldsymbol{q}^\flat)\ , \end{aligned} \tag{55}$$

where the last approximation $\approx$ holds due to (53). To explain:

$$\int_{t-\bar T}^t \dot\varphi(t-s)\mathrm{d}s = -\frac{\varphi_1}{\tau}\int_{t-T^\delta_\varphi}^t e^{-(t-s)/\tau}\mathrm{d}s = -\varphi_1(1-e^{-\bar T/\tau}) = \varphi(t-\bar t) - 1\ .$$

Let us recall that the steady state is attained far in the past, i.e. not later than for $t - \bar T = \bar t$.

Mass conservation. Due to the fading memory property and the steady state assumption we observe

$$\int_{t-\bar t}^t \dot\psi(t-s)\frac{\mathrm{d}}{\mathrm{d}\,s}\bar p(s)\mathrm{d}s \approx 0 \quad \text{ for } \quad t > \bar t + \bar T\ .$$

Therefore, (47) reduces to

$$\nabla\cdot\boldsymbol{K}\nabla p^\flat = 0 \quad \text{ in } \Omega\ , \tag{56}$$

To determine the steady state, obviously specific boundary conditions must be considered.

1. **Drained body.** Let $p^\flat = p_\Gamma$ be prescribed (constant w.r.t. time) on a nonempty segment $\Gamma \subset \partial\Omega$, whereas $\boldsymbol{n} \cdot \boldsymbol{W}^\flat = 0$ on the rest $\partial\Omega \setminus \Gamma$, see (45). Then (54), (55) and (56) yield a unique steady state solution $\boldsymbol{q}^\flat$.

2. **Undrained body.** We now have $\Gamma = \emptyset$, so that (56) with the homogeneous Neumann (nonpenetration) condition on the entire $\partial\Omega$ is satisfied by any constant $\bar{p}^\flat$. Assuming the impermeable boundary during all the history $t \in [-\infty, \bar{t}]$ and $p(-\infty) = 0$, we can find a unique pressure by integrating (47) in space and time: first we observe

$$0 = \int_\Omega \operatorname{div} \boldsymbol{W} = \int_\Omega (\phi \boldsymbol{I} + \boldsymbol{\beta}) : \dot{\boldsymbol{E}} + \int_\Omega (\phi\gamma + \hat{\mu})\dot{p} + \int_\Omega \hat{\mu} \int_{-\infty}^t \dot{\psi}(t-s) \frac{\mathrm{d}}{\mathrm{d}\, s} p(s) \mathrm{d}s \ . \quad (57)$$

To deal easily with the convolution integral, we can use again the Laplace transformation. Thus, using (43) multiplied by λ and recalling $\int_\Omega \operatorname{div} \boldsymbol{W} = 0$, we obtain

$$0 = \int_\Omega (\phi \boldsymbol{I} + \boldsymbol{\beta}) : \underset{*}{\boldsymbol{E}} + \int_\Omega \phi\gamma \underset{*}{p} + \int_\Omega \hat{\mu}\lambda\Psi(\lambda) \underset{*}{p} \ .$$

Hence using the inverse Laplace transformation and for $t > \bar{t} + \bar{T}$ (the steady state) we get

$$\begin{aligned} 0 &= \int_\Omega (\phi \boldsymbol{I} + \boldsymbol{\beta}) : \boldsymbol{E}^\flat + \int_\Omega (\phi\gamma + \hat{\mu}) p^\flat + \int_\Omega \hat{\mu} \int_{-\infty}^t \dot{\psi}(t-s) p(s) \mathrm{d}s \\ &\approx \int_\Omega (\phi \boldsymbol{I} + \boldsymbol{\beta}) : \boldsymbol{E}^\flat + \int_\Omega (\phi\gamma + \hat{\mu}\psi(t-\bar{t})) p^\flat \\ &\approx \int_\Omega (\phi \boldsymbol{I} + \boldsymbol{\beta}) : \boldsymbol{E}^\flat + \int_\Omega (\phi\gamma + \hat{\mu}\psi_0) p^\flat \ , \end{aligned} \quad (58)$$

where the last approximation holds by virtue of (53).

5.2 Modified problem of evolution with initial steady state

We now return to (51). To compute a response $\boldsymbol{q}(t) = \boldsymbol{q}^\flat + \boldsymbol{q}^\clubsuit(t)$ we can start at $t = 0$ with a given steady state $\boldsymbol{q}^\flat$ (the time is reset to zero assuming the steady state has been achieved) which is a unique solution $\bar{\boldsymbol{q}}^\flat = (\boldsymbol{U}^\flat, \bar{p}^\flat)$ satisfying (54) with $\boldsymbol{q}^\flat = \bar{\boldsymbol{q}}^\flat$ and $\bar{p}^\flat$ constrained by (58). On the steady state, at $t = 0$ we superimpose $\boldsymbol{q}^\clubsuit(t)$ which evolves from zero, i.e. we consider $\boldsymbol{q}^\clubsuit(0) = 0$.

Boundary conditions. In general, we may consider the following split (up to zero measure manifolds) of the boundary $\partial\Omega$:

$$\begin{aligned} \partial\Omega &= \partial_\sigma\Omega \cup \partial_u\Omega \ , \quad \partial_\sigma\Omega \cap \partial_u\Omega = \emptyset \ , \\ \partial\Omega &= \partial_w\Omega \cup \partial_p\Omega \ , \quad \partial_w\Omega \cap \partial_p\Omega = \emptyset \ . \end{aligned} \quad (59)$$

For simplicity, we shall consider the following boundary conditions:

$$\begin{aligned} \boldsymbol{U} &= 0 \quad \text{on } \partial_u\Omega \ , \\ \boldsymbol{n} \cdot \boldsymbol{S} &= \boldsymbol{\tau}_\partial \quad \text{on } \partial_\sigma\Omega \ , \\ p &= p_\partial \quad \text{on } \partial_p\Omega \ , \\ \boldsymbol{n} \cdot \boldsymbol{W} &= 0 \quad \text{on } \partial_w\Omega \ , \end{aligned} \quad (60)$$

where $\boldsymbol{n} = (n_i)$ is the unit normal outward to Ω and by subscript $\square_\partial$ we denote quantities prescribed on subsets of $\partial\Omega$.

Formal statement of the problem. Let us assume given volume forces $\boldsymbol{f}^\flat$, surface tractions $\boldsymbol{\tau}^\flat_\partial$ and pore fluid boundary pressure $p^\flat_\partial$. We define the *initial steady state* $\boldsymbol{q}^\flat = (\boldsymbol{U}^\flat, p^\flat)$ satisfying

$$\begin{aligned} -\nabla\cdot\Big[\varphi_0\mathbb{A}\boldsymbol{e}(\boldsymbol{U}^\flat) - (\phi\boldsymbol{I}+\boldsymbol{\beta})p^\flat\Big] &= \boldsymbol{f}^\flat \quad \text{in } \Omega\,, \\ \nabla\cdot\boldsymbol{K}\nabla p^\flat &= 0 \quad \text{in } \Omega\,, \end{aligned} \tag{61}$$

and the boundary conditions of the type (60) with $(\boldsymbol{U}, \boldsymbol{S}, p, \boldsymbol{W}) := (\boldsymbol{U}^\flat, \boldsymbol{S}^\flat, p^\flat, \boldsymbol{W}^\flat)$ where $p_\partial := p^\flat_\partial$ and $\boldsymbol{\tau}_\partial := \boldsymbol{\tau}^\flat_\partial$. We assume nonempty segments $\partial_u\Omega$ and $\partial_p\Omega$, i.e. the drained case is considered. Further let $\boldsymbol{f}(t,x)$ for $(t,x)\in[0,T]\times\Omega$ and $\boldsymbol{\tau}_\partial(t,x), p_\partial(t,x)$ for $(t,x)\in[0,T]\times\partial\Omega$ be given sufficiently smooth such that $(\boldsymbol{f}(0,\cdot),\boldsymbol{\tau}_\partial(0,\cdot),p_\partial(0,\cdot)) = (\boldsymbol{f}^\flat,\boldsymbol{\tau}^\flat_\partial,p^\flat_\partial)$. The solution of the *poro-visco-elastic problem* is a couple $(\boldsymbol{U},p)(t,x)$ for $(t,x)\in[0,T]\times\Omega$ satisfying the inital conditions $(\boldsymbol{U},p)(0,\cdot) = (\boldsymbol{U}^\flat,p^\flat)$, and the following equations

$$\begin{aligned} -\nabla\cdot\mathbb{A}\left[\boldsymbol{e}(\boldsymbol{U}(t)) + \int_0^t \dot\varphi(t-s)\boldsymbol{e}(\boldsymbol{U}(s))\mathrm{d}s + (\varphi_0-\varphi(t))\boldsymbol{e}(\boldsymbol{U}^\flat)\right] & \\ +\nabla\cdot(\phi\boldsymbol{I}+\boldsymbol{\beta})p(t) = \boldsymbol{f}(t) \quad \text{in }]0,T]\times\Omega\,, & \\ (\phi\boldsymbol{I}+\boldsymbol{\beta}):\boldsymbol{e}(\dot{\boldsymbol{U}}(t)) - \nabla\cdot\boldsymbol{K}\nabla p(t) & \\ +(\phi\gamma+\hat\mu)\dot p(t) + \hat\mu\int_0^t\dot\psi(t-s)\dot p(s)\mathrm{d}s = 0 \quad \text{in }]0,T]\times\Omega\,, & \end{aligned} \tag{62}$$

and the boundary conditions (60) for $t\in]0,T]$.

It can be shown that formulation (62) is consistent with the model (46),(47) derived for the zero initial conditions and with the steady state superposition (51). First we notice that $(62)_2$ holds whenever the couple $(\boldsymbol{U}^\clubsuit, p^\clubsuit)$ satisfies the balance of mass in (47) and $p^\flat$ satisfies (56). To prove also the consistency of the equilibrium equation $(62)_1$ in the sense of the decomposition (51), we use the following identity which holds for $\varphi(t)$ defined in (14),

$$\int_0^t\dot\varphi(t-s)\mathrm{d}s = -\frac{\varphi_1}{\tau}\int_0^t e^{-(t-s)/\tau}\mathrm{d}s = -\varphi_1(1-e^{-t/\tau})\,. \tag{63}$$

Hence, by virtue of (51)

$$\int_0^t\dot\varphi(t-s)\boldsymbol{e}(\boldsymbol{U}(s))\mathrm{d}s = -\varphi_1(1-e^{-t/\tau})\boldsymbol{e}(\boldsymbol{U}^\flat) + \int_0^t\dot\varphi(t-s)\boldsymbol{e}(\boldsymbol{U}^\clubsuit(s))\mathrm{d}s\,. \tag{64}$$

Recalling $\varphi_0+\varphi_1=1$, thereby

$$[1-\varphi_1(1-e^{-t/\tau})]\boldsymbol{e}(\boldsymbol{U}^\flat) = (\varphi_0+\varphi_1e^{-t/\tau})\boldsymbol{e}(\boldsymbol{U}^\flat) = \varphi(t)\boldsymbol{e}(\boldsymbol{U}^\flat)\,,$$

we can rewrite the first bracketed left hand side term in (62)

$$\begin{aligned} &\boldsymbol{e}(\boldsymbol{U}(t)) + \int_0^t\dot\varphi(t-s)\boldsymbol{e}(\boldsymbol{U}(s))\mathrm{d}s + (\varphi_0-\varphi(t))\boldsymbol{e}(\boldsymbol{U}^\flat) \\ =&\boldsymbol{e}(\boldsymbol{U}^\clubsuit(t)) + \int_0^t\dot\varphi(t-s)\boldsymbol{e}(\boldsymbol{U}^\clubsuit(s))\mathrm{d}s + (\varphi_0+\varphi_1e^{-t/\tau})\boldsymbol{e}(\boldsymbol{U}^\flat) + (\varphi_0-\varphi(t))\boldsymbol{e}(\boldsymbol{U}^\flat) \\ =&\boldsymbol{e}(\boldsymbol{U}^\clubsuit(t)) + \int_0^t\dot\varphi(t-s)\boldsymbol{e}(\boldsymbol{U}^\clubsuit(s))\mathrm{d}s + \varphi_0\boldsymbol{e}(\boldsymbol{U}^\flat)\,. \end{aligned} \tag{65}$$

Hence, by defining $\boldsymbol{f}(t) = \boldsymbol{f}^\flat + \boldsymbol{f}^\clubsuit(t)$ with $\boldsymbol{f}^\clubsuit(0) = 0$, we see that (62) holds for $(\boldsymbol{U}^\clubsuit, p^\clubsuit)$ which solves

$$-\nabla \boldsymbol{S}^\clubsuit(t) = \boldsymbol{f}^\clubsuit(t)\ , \quad \boldsymbol{S}^\clubsuit(t) \text{ defined according to (46)}\ ,$$

with (47) written for $(\boldsymbol{U}^\clubsuit, p^\clubsuit)$, whereas $(\boldsymbol{U}^\flat, p^\flat)$ satisfies the steady state problem (61). This completes the consistency proof.

6 Conclusions

Using some ideas of a micromechanical analysis we have developed a model of a viscoporoelastic material formed by a viscoelastic skeleton with connected porosity. The structure of the homogenized model attains the form of the Biot model extended by some fading memory terms in the stress and pressure equations.

For the solid material we considered a viscoelastic constitutive law defined in terms of a scalar relaxation function φ, so that the exponential decay associated to the relaxation is synchronous for all stress components. In the upscaled medium, it was shown that the fading memory phenomenon features the stress–strain relationship by virtue of the same relaxation function, whereas the part of the Biot compressibility which is induced by the skeleton properties incorporates the creep function ψ associated to φ. The Biot stress coefficients coupling strains and the fluid pressure are not affected by the solid viscosity. The model has been implemented using a discrete time mixed and Galerkin finite element method in [39] where stability and *a priori* error estimates are also derived.

Although a classical periodic homogenization can be performed using asymptotic analysis, here we obtained the homogenized model using a less rigorous procedure based on averaging over the RVE and assuming ad hoc scale separation. This approach, however, leads to the two-scale model such that the homogenized material coefficients can be computed for a given geometry of the microstructure. Moreover, this approach can be extended formally, in much the same way as in e.g. [32, 35], also for nonlinear problems arising along with large deformations or material nonlinearities, cf. [15].

In the present paper we assumed only moderate pressure gradients on the macroscopic scale leading to slow flows in the microstructures without any pressure fluctuation on the pore scale.

As a result we were able to simplify the fluid-structure interaction in the microstructure by neglecting fluid velocity and wall shear stresses, see [37] where similar treatment was employed for a two-level upscaling procedure. If we were to consider dynamic effects, however, such simplification would not be possible. An extension to this case will be considered in a later work. We note here that Showalter and Stefanelli [41] began this study but concentrated mainly on plasticity effects in the solid. Also, Clopeau et al [11], Ferrín & Mikelic, [18], Auriault & Boutin, [6] and Mielke & Rohan [27] provide excellent starting points with their studies of elastic solids.

As a next step one may consider an extension of the perfusion models based on the micro-macro analysis and homogenization [33] to include the viscoelastic behaviour of the solid phase. In effect, recalling our discussion in the Introduction, such a homogenized model would feature fading memory phenomena arising on one hand due to the microflows in the dual porosity, which leads to the convolution integrals associated with all effective coefficients (see [38] and also [34] for a numerical scheme) and, on the other hand, due to the solid skeleton viscoelasticity, as discussed in this work.

Acknowledgment. The research of the first author is supported in part by project "IGA", NT 13326 of the Ministry of Health of the Czech Republic, by the European Regional Development Fund (ERDF), project "NTIS - New Technologies for Information Society", European Centre of Excellence, CZ.1.05/1.1.00/02.0090 and by project SGS-2013-026. The research of J. R. Whiteman was supported in part by J. T. Oden Fellowships that enabled him to spend several periods at ICES, Institute of Computational Engineering and Sciences at the University of Texas at Austin. All this support is gratefully acknowledged.

References

[1] Y. N. Abousleiman, A. H.-D. Cheng, and J. C. Roegiers. Poroviscoelastic analysis of borehole and cylinder problems. *Acta Mechanica*, 119:199–219, 1996.

[2] G. Allaire. Homogenization of the stokes flow in a connected porous medium. *Asymptotic Analysis*, 2:203–222, 1989.

[3] G. Allaire. Homogenization and two-scale convergence. *SIAM J. Math. Anal.*, 23:1482–1518, 1992.

[4] T. Arbogast, J. Douglas, and U. Hornung. Derivation of the double porosity model of single phase flow via homogenization theory. *SIAM J. Math. Anal.*, 21:823–836, 1990.

[5] J.-L. Auriault and C. Boutin. Deformable porous media with double porosity. quasi statics. ii. memory effects. *Transp. Porous Media*, 10(2):153–169, 1993.

[6] J.-L. Auriault and C. Boutin. Deformable porous media with double porosity iii. acoustics. *Transp. Porous Media*, 14:143–162, 1994.

[7] M. A. Biot. Mechanics of deformation and acoustic propagation in porous media. *J Applied Physics*, 33:1482–1498, 1962.

[8] A. Blasselle and G. Griso. Mechanical modeling of the skin. *Asymptotic Analysis*, 74:167–198, 2011.

[9] James Case. Recreating the great San Francisco earthquake. *SIAM News*, 42(3):1,8, April 2009. (News journal of the Society for Industrial and Applied Mathematics).

[10] D. Cioranescu, A. Damlamian, and G. Griso. The periodic unfolding method in homogenization. *SIAM Journal on Mathematical Analysis*, 40(4):1585–1620, 2008.

[11] T. Clopeau, J.L. Ferrin, R.P. Gilbert, and A. Mikelic. Homogenizing the acoustic properties of the seabed: Part ii. *Mathematical and Computer Modelling*, 33:821–841, 2001.

[12] O. Coussy. *Poromechanics*. John Wiley & Sons, 2004.

[13] R. de Boer. *Theory of Porous Media*. Springer, Berlin, 2000.

[14] P. de Buhan, X. Chateau, and L. Dormieux. The constitutive equations of finite strain poroelasticity in the light of a micro-macro approach. *Eur. J. Mech. A/Solids*, 17:909921, 1998.

[15] L. Dormieux, A. Molinari, and D. Kondo. Micromechanical approach to the behavior of poroelastic materials. *Jour. Mech. Phys. Solids*, 50:2203–2231, 2002.

[16] W. Ehlers and J. Bluhm. *Porous Media, Theory, Experiments and Numerical Applications*. Springer, 2002.

[17] W. Ehlers, B. Markert, and O. Klar. Biphasic description of viscoelastic foams. In *Porous Media, Theory, Experiments and Numerical Applications*, pages 275–294. Springer, 2002.

[18] J.L. Ferrín and A. Mikelić. Homogenizing the acoustic properties of a porous matrix containing an incompresssible inviscid fluid. *Math. Meth. Appl. Sci.*, 26:831–859, 2003.

[19] R.P. Gilbert and A. Mikelić. Homogenizing the acoustic properties of the seebed: Part i. *Nonlinear Analysis*, 40:185–212, 2000.

[20] J. M. Golden and G. A. C. Graham. *Boundary value problems in linear viscoelasticity*. Springer-Verlag, 1988.

[21] G. Griso and E. Rohan. On the homogenization of a diffusion-deformation problem in strongly heterogeneous media. *Ricerche mat.*, 56:161–188, 2007.

[22] R. Hill. Elastic properties of reinforced solids: Some theoretical principles. *J. Mech. Phys. Solids*, 11:357–372, 1963.

[23] R. Hill. The essential structure of constitutive laws for metal composites and polycrystals. *J. Mech. Phys. Solids*, 15:79–95, 1967.

[24] S. K. Hoag, Y. N. Abousleiman, and T. Hemphill. Poroviscoelastic modelling of time-dependent wellbore closure when drilling anisotropic gas shale and oil shale reservoirs – applications in the haynesville shale and the colony pilot mine shale. *Society of Petroleum Engineers SPE159942*, 2012.

[25] U. Hornung. *Homogenization and porous media*. Springer, Berlin, 1997.

[26] V. Lukeš and E. Rohan. Microstructure based two-scale modelling of soft tissues. *Math. and Computers in Simulation*, 65(215):1019–1037, 1996.

[27] A. Mielke and E. Rohan. Homogenization of elastic waves in fluid-saturated porous media using the Biot model. *Math. Models and Meth. in Appl. Sci.*, 23:873–916, 2013.

[28] A. Mikelić. Mathematical derivation of the darcy-type law with memory effects, governing transient flow through porous medium. *Glasnik Matematickij*, 29:57–77, 1994.

[29] S. Nemat-Nasser and M. Hori. *Micromechanics: Overall Properties of Heterogeneous Materials*. Series in Applied Mathematics and Mechanics. North-Holland, 1993.

[30] D. Perić, E.A. de Souza Neto, R. Feijóo, and A.J. Carneiro Molina. On micro-to-macro transitions for multi-scale analysis of non-linear heterogeneous materials: unified variational basis and finite element implementation. *I. Jour. Num. Meth. Engrg.*, 87:149170, 2010.

[31] F. M. Rago, H. Ockuma, K. Sepehrnoori, and T. W. Thompson. Reservoir performance in viscoelastic porous media. *J. Engrg. Resources Technology*, 107:527–533, 1985.

[32] E. Rohan. Modelling large deformation induced microflow in soft biological tissues. *Theor. and Comp. Fluid Dynamics*, 20:251–276, 2006.

[33] E. Rohan and R. Cimrman. Two-scale modelling of tissue perfusion problem using homogenization of dual prous media. *Int. Jour. for Multiscale Comput. Engrg.*, 8:81–102, 2010.

[34] E. Rohan and R. Cimrman. Multiscale FE simulation of diffusion-deformation processes in homogenized dual-porous media. *Math. Comp. Simul.*, 82:1744–1772, 2012. In Press.

[35] E. Rohan, R. Cimrman, and V. Lukeš. Numerical modelling and homogenized constitutive law of large deforming fluid saturated heterogeneous solids. *Computers and Structures*, 84:1095–1114, 2006.

[36] E. Rohan and V. Lukeš. Homogenization of perfusion in large-deforming medium using the updated lagrangian formulation. In *Proceedings of the ECT 2010 conference*. Coburg-Sax Publ., 2010.

[37] E. Rohan, S. Naili, R. Cimrman, and T. Lemaire. Hierarchical homogenization of fluid saturated porous solid with multiple porosity scales. *Comptes Rendus Mecanique*, 340:688–694, 2012.

[38] E. Rohan, S. Naili, R. Cimrman, and T. Lemaire. Multiscale modelling of a fluid saturated medium with double porosity: Relevance to the compact bone. *Jour. Mech. Phys. Solids*, 60:857–881, 2012.

[39] E. Rohan, S. Shaw, M. F. Wheeler, and J. R. Whiteman. Mixed and Galerkin finite element approximation of flow in a linear viscoelastic porous medium. Technical report, BICOM, Brunel University, 2012. Technical Report 12/2, `www.brunel.ac.uk/bicom`.

[40] E. Sanchez-Palencia. *Non-homogeneous media and vibration theory*. Number 127 in Lecture Notes in Physics. Springer, Berlin, 1980.

[41] R.E. Showalter and U. Stefanelli. Diffusion in poro-plastic media. *Math. Meth. Appl. Sci.*, 27:2131–2151, 2003.

[42] R.E. Showalter and D.B. Visarraga. Double-diffusion models from a highly heterogeneous medium. *Journal of Mathematical Analysis and Applications*, 295:191–210, 2004.